Demonstration and optical characteristics of electro-optic Bragg modulators in periodically poled lithium niobate in the near-infrared

J. A. Abernethy, C. B. E. Gawith, R. W. Eason, and P. G. R. Smith[a)]
Optoelectronics Research Centre, University of Southampton, Southampton, S017 1BJ, United Kingdom

(Received 8 May 2002; accepted 6 August 2002)

We report the infrared operation of a bulk optical Bragg modulator based on electro-optically induced refractive index gratings in *z*-cut periodically poled lithium niobate. Efficiencies in the first order of 45% for 1064 nm *e*-polarized light and 30% for *o*-polarized light were achieved, with maximum on/off ratios of 15:1 and 9:1, respectively. Field-induced light scattering effects due to poling are observed at higher drive voltages and compromised device performance due to these scattering effects is predicted to limit long-wavelength operation of these devices. © *2002 American Institute of Physics.* [DOI: 10.1063/1.1510964]

Many successful technologies exist for laser modulators including acousto-optic and bulk electro-optic devices. However, recently another class of modulators, based on Bragg diffraction in periodically poled materials, has attracted attention.[1,2] Their advantages include lower drive voltages and faster response times than conventional types. These devices are an extension of early work on grating based electro-optic devices such as those by Hammer[3] and Barros,[4] but by making use of periodic poling they allow additional design freedom.

Bragg grating devices based on periodically poled $LiNbO_3$ (PPLN) were first investigated by Yamada[1] and Gnewuch[2] using visible light at 633 nm, and again by Yamada[5] using violet-blue light at 407 nm. Impressive maximum first order diffraction efficiencies of around 75% were reported by both authors. Gnewuch *et al.* demonstrated a fivefold reduction in switching time compared to acousto-optic devices, and also that periodic poling suppresses acoustic modes excited via the piezoelectric effect by the electrode capacitance.[6] Yamada *et al.* demonstrated several different optical functions using electro-optically controlled PPLN, such as focussing, switching, and deflecting, and confirmed that these fundamental operations may be integrated on the same substrate. More recently, Yamada *et al.* presented results for Bragg gratings used as an optical switch with one input and six outputs, and as a wide band optical modulator for violet-blue light.[5]

In this letter we present results on PPLN-based electro-optic Bragg modulators operating at 1064 nm, describe their fabrication, and discuss operating considerations for such devices. We present results of field induced scattering at higher drive voltages, an effect found to result from the periodic-poling process, and our initial investigation of reduced device efficiency at 1064 nm when compared to visible operation. Light redistribution into higher orders and in-plane scatter are measured, and compromised performance at longer wavelengths due to this scatter is predicted.

A PPLN-based Bragg modulator device consists of an area of periodically domain inverted regions forming a grating of length, d, and of period, Λ, with grating k-vector parallel to the x axis of the crystal, an arrangement illustrated in Fig. 1. The devices used in this experiment were fabricated from 500-μm-thick z-cut lithium niobate purchased from Yamaju Ceramics Co. Ltd, and processed such that a grating was photolithographically patterned on the $-z$ face before domain inversion at room temperature using a liquid-gel electrode technique.[7] A top strip electrode and a bottom ground plate were formed by depositing aluminum on the $+z$ and $-z$ faces of the device, the y faces of which were then parallel polished to optical flatness. By applying a uniform electric field, E, between the two electrodes a periodic refractive index change of amplitude

$$\Delta n = -n_0^3 r_{ij} E_z/2 \tag{1}$$

can then be induced. The largest electro-optic coefficient in lithium niobate is accessed by extraordinary (e) polarized light as shown in Fig. 1, with a value (at 633 nm) of $r_{33} = 32.2\times10^{-12}$ mV^{-1}. With o-polarized light the electro-optic coefficient $r_{13} = 8.6\times10^{-12}$ mV^{-1} is used.[8]

While a full theoretical analysis for the operation of a PPLN-based Bragg modulator device is complex, a good quantitative agreement can be obtained by using a simple model based on a thick sinusoidal grating.[9] The first order diffraction efficiency of such a thick Bragg grating is given by the equation

$$\eta = \sin^2(\pi \Delta n d/\lambda \cos\theta), \tag{2}$$

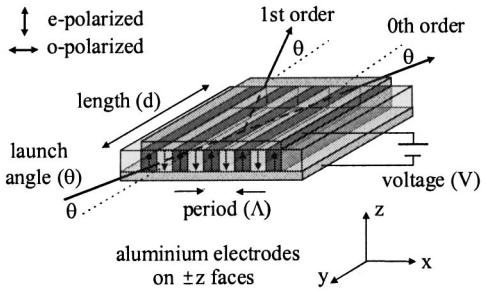

FIG. 1. Schematic diagram of a periodically poled $LiNbO_3$ Bragg modulator device.

a)Electronic mail: pgrs@orc.soton.ac.uk

where η is the diffraction efficiency, λ is the wavelength in free space, θ is the internal angle between the incident light and y axis of the crystal, d is the length of the grating, and Δn is the change in refractive index due to the applied field. This efficiency equation only holds if the Bragg relation

$$\sin\theta = \lambda/2n\Lambda \tag{3}$$

is satisfied, where Λ is the period of the grating. For a given grating period a large range of wavelengths can satisfy this equation by alteration of the launch angle, such that the only constraints on the operating conditions are set by the device geometry. This means that, once fabrication constraints have been taken into account, it should be possible to design a device that would give high theoretical diffraction efficiencies at any given wavelength.

It should be noted that in the real case the induced refractive index profile is far from sinusoidal and follows a pattern closer to that of a square wave. However, while this refractive index structure can be Fourier decomposed into many finer period sinusoidal gratings, which would in turn cause scattering of the incident beam into several higher orders, these higher-order diffracted spots are not Bragg-matched and therefore contain only a small fraction of power from the incident beam. Separate numerical diffraction calculations based on devices operating in the low conversion regime support this assertion, with higher-order beams being orders of magnitude weaker than that of the first-order interaction.

Characterization of the PPLN-based Bragg modulator devices was performed in the infrared using a Nd:YAG laser operating at a wavelength of 1064 nm, and in the visible using a He:Ne laser at 633 nm and argon-ion laser at 488 nm. In each case the beam was passed through a polarizing beam splitter and half wave plate to allow polarization control, and then focused into the device using a 300 mm lens. The sample was mounted on a 5-axis micropositioner to allow movement in the x, y, and z axes, and also tilt about the center of the sample in the $x-y$ plane and the $y-z$ plane. The required incident angle for Bragg matching was then set using the micropositioner. A signal generator provided the required voltage wave form, which was then amplified and applied to the top and bottom electrodes on the sample. The range of voltages available for this experiment was ± 200 V, as determined by the maximum working range of the voltage amplifier (NewFocus model 3211). Calibrated photodiode detectors were positioned at the output of the zero and first diffracted orders and pinholes were used to eliminate any background signal. The output from each detector was passed to an oscilloscope for comparison and recording.

The operation of a Bragg grating modulator at 1064 nm for both e- and o-polarized light is demonstrated in Fig. 2. The PPLN device used for this experiment featured a 3 cm long grating with a 70 μm period, and an incident beam power of 53 mW was used. Operating conditions based on this device geometry correspond to a theoretical internal Bragg angle of 0.19°, and an external angle, via Snell's Law, of 0.44°. In practice, the external angle for maximum diffraction efficiency was measured to be 0.4° ($\pm 0.25°$), which is in agreement with this figure. From the diagram, an approximate fit between the scaled theoretical diffraction efficiency calculated using Eq. (2) (illustrated as the dashed curves of Fig. 2) and measured efficiency (the solid curves) is evident, especially for lower drive voltages. The theory is scaled to the maximum experimental efficiency in each case.

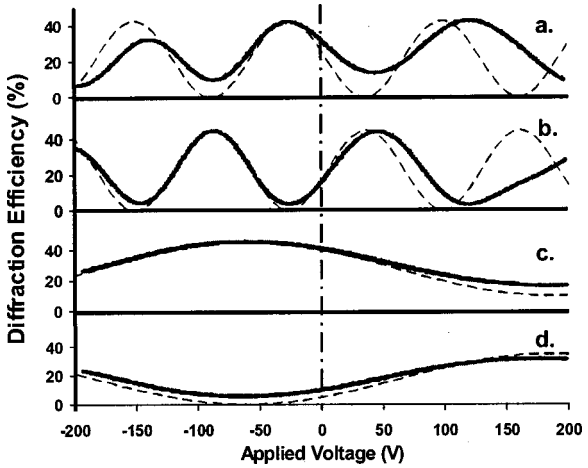

FIG. 2. Graph of diffraction efficiency vs applied voltage. Dashed lines represent the scaled theoretical diffraction efficiency and solid lines represent the measured data for; (a) zeroth order diffraction with e-polarized light, (b) first order diffraction with e-polarized light, (c) zeroth order diffraction with o-polarized light, and (d) first order diffraction with o-polarized light.

On/off voltages of 65 V for e-polarized light and 225 V for o-polarized light were measured and diffraction efficiencies in the first order of 45% for e-polarized light and 30% for o-polarized light are determined from Fig. 2. On/off ratios in the first order of 15:1 for e-polarized and 9:1 for o-polarized light and off/on ratios in the zeroth order of 7:1 for e-polarized and 5:1 for o-polarized light were achieved. In addition, Fig. 2 demonstrates that for operation with e-polarized light the effective zero field point occurs at a driving voltage of -27 V and not 0 V. It is believed that the origin of this offset is due to a residual refractive index grating that remains after the periodic-poling process, a phenomenon also reported by other groups.[5] Annealing of the device has been found to reduce this effect, but does not fully alleviate the problem.

In keeping with data we have taken at shorter wavelengths, higher field maxima [corresponding to higher orders in the argument of Eq. (2) (π, 3π, 5π...)] have been found to exhibit lower diffraction efficiencies. It was also discovered that the diffraction efficiencies achieved when operating in the infrared were consistently lower than for visible operation. Such reduced efficiency is attributed to two effects, the first of which is the scattering of some optical power into higher order spots due to imperfections along the poled grating structure, and the second a voltage induced scatter at increased drive voltages. The latter effect is inherently increased for infrared operation, as the on/off voltages required are higher than those for visible operation.

In order to investigate power redistribution into higher order diffracted spots, and to measure general scatter and beam degradation, angularly resolved beam measurements were performed by scanning a photodetector across the diffracted output peaks of the device. As is clearly demonstrated both theoretically and experimentally in Fig. 2, the

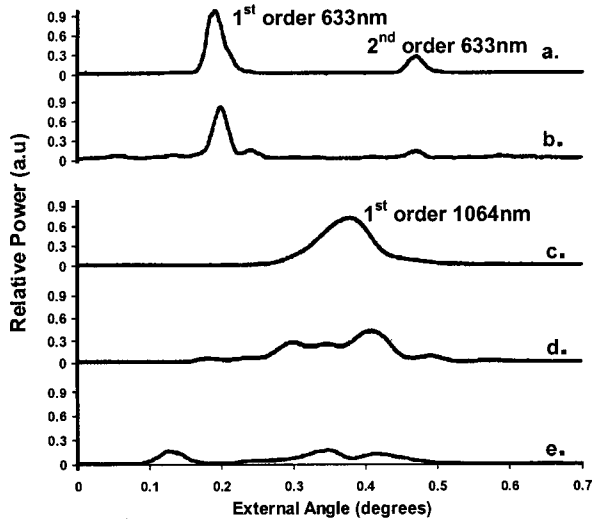

FIG. 3. Line scans at peaks of maximum diffraction into the first order for *e*-polarized light, showing; (a) visible light (633 nm) at low field peak of $-40\ \mathrm{V\,mm^{-1}}$, (b) visible light (633 nm) at high field peak of $-160\ \mathrm{V\,mm^{-1}}$, (c) infrared light (1064 nm) at low field peak of $+90\ \mathrm{V\,mm^{-1}}$, (d) infrared light (1064 nm) at medium field peak of $-180\ \mathrm{V\,mm^{-1}}$, and (e) infrared light (1064 nm) at high field peak of $-460\ \mathrm{V\,mm^{-1}}$.

first-order diffraction efficiency maximizes periodically with increases in the applied field. Comparison of the diffraction characteristics of successive first-order peaks then allows investigation of voltage-induced scatter with respect to increased applied field. Figure 3 shows angularly resolved line scans taken at incident wavelengths of 633 and 1064 nm for successive field strength first-order peaks. At higher voltages the output beam quality is clearly degraded, such that the diffraction efficiency from the zero to first order is reduced, accompanied by an increased scatter of power into the higher orders and background. Under infrared operation, this background scatter represents the major cause of power redistribution from the first-diffracted order, as the higher order spots contain relatively little of the initial input power. As the scattering and beam degradation in the poled regions of the device is dramatically stronger than that of the unpoled reference areas under the same applied field, we can confidently associate this scatter with the poling process used to fabricate the gratings. It should be noted, however, that the voltage induced scatter does not appear to depend on poling quality, and is more likely due to the inherent presence of domain walls within the structure.

In conclusion, we have reported the fabrication and near-infrared operation of a periodically poled lithium niobate Bragg electro-optic modulator device. Characterization of a 3 cm long device with a 70 μm grating period provided diffraction efficiencies of 44% for *e*-polarized light and 30% for *o*-polarized light at an operational wavelength of 1064 nm. It was observed that the higher drive fields required at longer wavelengths lead to reduced diffraction efficiencies, an investigation of which revealed the primary cause as voltage induced scatter at domain walls. This effect was confirmed with angularly resolved line scan measurements, which show that diffraction efficiencies are reduced at higher voltages due to beam degradation and increased background scatter at higher applied fields. Such results demonstrate that while Bragg modulators based on periodically poled materials have a high degree of flexibility in terms of design and operating conditions, some operating restrictions apply for high diffraction efficiency, favoring visible operation with its lower on/off voltages. However, as beam degradation is clearly an intrinsic effect due to the poling process, it may be possible to reduce this effect in materials that can be poled with a much lower coercive field, such as stochiometric lithium niobate.[10]

[1] M. Yamada, M. Saitoh, and H. Ooki, Appl. Phys. Lett. **69**, 3659 (1996).
[2] H. Gnewuch, C. N. Pannell, G. W. Ross, P. G. R. Smith, and H. Geiger, IEEE Photonics Technol. Lett. **10**, 1730 (1998).
[3] J. M. Hammer, Appl. Phys. Lett. **18**, 147 (1971).
[4] M. A. R. P. Barros and M. G. F. Wilson, Electron. Lett. **7**, 267 (1971).
[5] M. Yamada, Rev. Sci. Instrum. **71**, 4010 (2000).
[6] P. Basseras, R. J. D. Miller, and S. M. Gracewski, J. Appl. Phys. **69**, 7774 (1991).
[7] J. Webjorn, V. Pruneri, P. St. J. Russell, J. R. M. Barr, and D. C. Hanna, Electron. Lett. **30**, 894 (1994).
[8] R. S. Weis and T. K. Gaylord, Appl. Phys. A: Solids Surf. **A37**, 191 (1985).
[9] H. Kogelnik, Bell Syst. Tech. J. **48**, 2909 (1969).
[10] K. Kitamura, S. Takekawa, M. Nakamura, and Y. Furukawa, CLEO/PR Chiba, WH2-1, 2001.